

Sensing Performance of a ZnO-based Ammonia Sensor

Dinesh Kumar Chaudhary^{1,2}, Yogesh Singh Maharjan¹, Sanju Shrestha², Surendra Maharjan³, Shankar Prasad Shrestha⁴ and Leela Pradhan Joshi^{1*}

¹Department of Physics, Amrit Campus, Tribhuvan University, Kathmandu 44600, Nepal

²Central Department of Physics, Tribhuvan University, Kirtipur, Kathmandu 44618, Nepal

³Department of Physics, University of Houston, Houston, TX 77204, USA

⁴Department of Physics, Patan Multiple Campus, Tribhuvan University, Kathmandu 44700, Nepal

*Corresponding author: leela.pradhanjoshi@ac.tu.edu.np

Published online: 25 April 2022

To cite this article: Chaudhary, D. K. et al. (2022). Sensing performance of a ZnO-based ammonia sensor. *J. Phys. Sci.*, 33(1), 97–108. <https://doi.org/10.21315/jps2022.33.1.7>

To link to this article: <https://doi.org/10.21315/jps2022.33.1.7>

ABSTRACT: *Monitoring and remediation of toxic and flammable gases have become a critical task for the development of a clean society. Among various types of metal oxide semiconductors (MOS), zinc oxide (ZnO) is considered a potential material for gas sensing application because of its high sensitivity, easy synthesis, and high thermal stability behaviours. This research aimed to gain an in-depth understanding of the sensing task of a very stable and porous thin film of spin coated ZnO for detecting toxic ammonia vapour at room temperature. As-prepared ZnO films were characterised by x-ray diffraction (XRD), scanning electron microscopy (SEM), and ultraviolet-visible (UV-vis) analyses. XRD and SEM results revealed the polycrystalline wurtzite ZnO phase with grainy surface morphology. Optical calculations quantify the direct band gap of ZnO as 3.2 eV. The sensitivity measurements showed a good response ratio of 38.5 ± 0.6 with an exposure of 400 ppm of ammonia vapour. The results on sensitivity measurement of several cycles illustrated its stability and sensing performance better than other reported similar works. These findings will be useful to develop a low cost and efficient room temperature MOS gas sensor that can efficiently detect extremely low concentrations as 20 ppm of ammonia vapour which is below the Occupational Safety and Health Administration (OSHA) recommended value.*

Keywords: zinc oxide, sensor, response time, band gap, ammonia

1. INTRODUCTION

Detecting and being aware of the presence of toxic gases in the environment and leakages in occupational places are important and major priorities for safety and wellbeing. Among many other toxic gases, ammonia (NH_3) is one of the widely used in industrial sectors.¹⁻³ According to the Occupational Safety and Health Administration (OSHA) guidelines, personal exposure of NH_3 with a lower limit of up to 35 ppm for continuous 8 h and an upper limit of up to 50 ppm for 5 min cause severe health hazards. This threshold limit directly influences personal wellbeing as well. Ammonia sensors are highly promising in identifying gas spillage and leakage in a controlled atmosphere at room temperature in various sectors like agriculture, pharmaceutical, automotive, defence and food processing.⁴⁻⁶ In recent times, experimentalists considered zinc oxide (ZnO) as a promising metal oxide material due to its amazing features like high chemical and thermal stability, wide band gap (3.00 eV–3.24 eV), easy tunability of its structural, optical, electrical, and electronic properties.⁷⁻¹⁰ Though ZnO has been utilised for sensing various gases, it has some drawbacks such as high working temperature ($>200^\circ\text{C}$), poor selectivity, and relatively low response.⁶ The operation of a metal oxide semiconductors (MOS) gas sensor at high temperatures affects its stability and consumes power.⁹ Therefore, the fabrication of a room temperature MOS gas sensor is advantageous for improving long-term stability and low power consumption. A number of research are going on to overcome these problems.¹¹ In this work, we report the gas sensing efficacies, selectivity, and detection limit of spherical grainy structured spin-coated ZnO thin film-based sensors towards ammonia vapour at room temperature. We also report in-depth sensing characteristics like sensitivity, response and recovery times, and reproducibility of ZnO films.

2. EXPERIMENTAL

2.1 Deposition of ZnO Film

Thin films of ZnO were deposited on glass substrates using a 0.35 M precursor solution of zinc acetate, ethanol, and diethanolamine. The analytical grades of precursor materials were purchased from Merck (China) and used without further purification. The mixture was stirred for 1 h at 70°C until the solution is clear and homogeneous which was subsequently filtered using a Whatman filter paper and left for 24 h at room temperature.¹⁰ The spin coating recipe was set to 30 s of spinning at a rate of 3000 rpm for each layer of deposition. The adherent layer

was then soft-baked at 130°C for 5 min, followed by hard-bake at 400°C for 10 min. Finally, the sample was annealed at 450°C for 1 h inside the muffle furnace.⁷

2.2 Sensor Setup

Figure 1 shows the schematic representation of the gas sensing setup used in this work. It consists of two chambers, a left chamber, where ammonia vapour is created by heating liquid ammonia above its boiling point which interconnects with the right test chamber. A digital temperature controller hot plate (TALBOYS 7X7 CER HP 230 V ADV, by Henry Troemner, LLC, USA) was used to set the temperature hot plate at (120 ± 4) °C. The test chamber has three openings for gas inlet, air inlet, and outlet. The ZnO sensor is retrofitted inside the test chamber to measure its response at exposure to different concentrations of ammonia. The sensitivity of the gas sensor was measured in terms of current measured at two different environments using $R = \frac{I_g}{I_a}$ where I_a and I_g are the currents flowing through the ZnO in air and gas, respectively.¹²

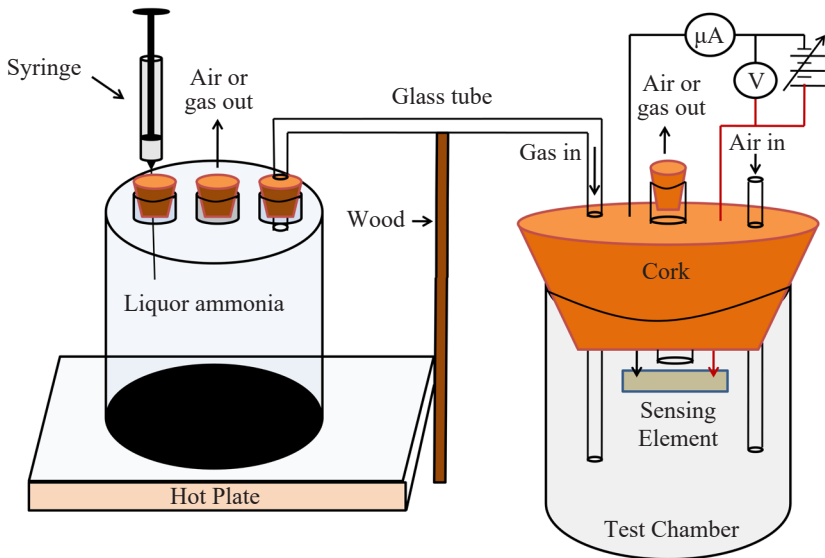


Figure 1: Schematic diagram of a gas sensor setup.

3. RESULTS AND DISCUSSION

3.1 Structural Analysis

Structural examination of ZnO thin films was done using the x-ray diffraction (XRD) technique. Figure 2 shows the XRD of spin coated ZnO in the 2θ from 20° – 80° using Cu- K_α radiation of wavelength 1.54056 \AA with a Bruker AXS, D2 PHASER A26-X1-A2BOB2A-, Serial No: 207047 diffractometer. The presence of multiple sharp peaks in the XRD pattern of spin-coated ZnO thin film reveals the polycrystalline nature of ZnO film. Major sharp peaks observed at $2\theta = 31.8627^\circ$, 34.5092° , 36.3202° , 47.5594° , 56.3553° , 62.7889° , 67.8320° and 68.9580° correspond to (100), (002), (101), (102), (110), (103), (112) and (201), respectively, which were found to be consistent with standard values of JCPDS card No., 36-1451.¹³ No additional impurity peak was observed which ensures the formation of pure ZnO. The crystallite size (D) was determined

using Debye Scherer's formula $D = \frac{0.94\lambda}{\beta \cos \theta}$ where 0.94 is the correction factor,

λ is the x-ray, wavelength and β and θ represent the full width at half maximum (FWHM) and diffraction angle, respectively.^{14,15} Likewise, the lattice strain (ϵ)

of ZnO film was calculated using the formula, $\epsilon = \frac{\beta}{4 \tan \theta}$.^{9,16} The average D and

ϵ were found to be $(27.60 \pm 0.86) \text{ nm}$ and $(3.16 \pm 0.28) \times 10^{-3}$, respectively.

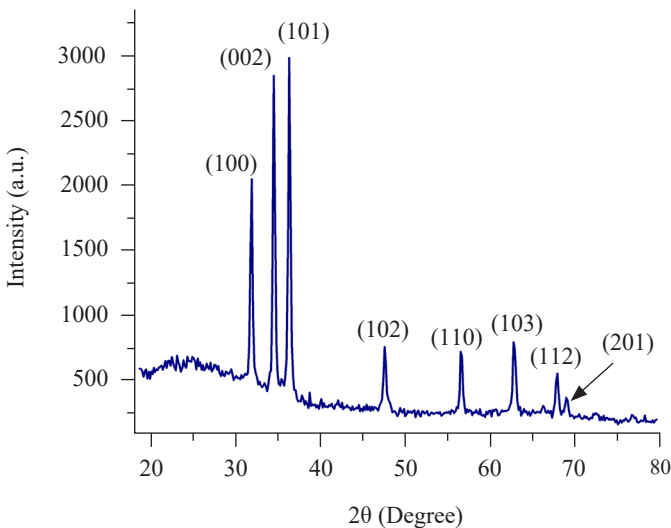


Figure 2: X-ray diffraction pattern of ZnO film.

3.2 Optical Band Gap

Figure 3(a) represents the UV-vis transmission spectrum of the ZnO sample in the wavelength range 300 nm–1000 nm at room temperature captured using a HR4000CG UV-NIR Ocean Optics (Singapore) spectrophotometer. The optical transmittance of ZnO film was more than 80% in the visible region. We notice a sharp decrease in transmittance at shorter wavelengths near the ultraviolet range which is typical in ZnO.¹⁷ The optical band gap was determined from transmittance data using a Tauc plot, described by $(\alpha h\nu)^2 = A(h\nu - E_g)$ where α , A , $h\nu$ and E_g are the absorption coefficient, energy constant, photon energy and optical band gap, respectively. The extrapolation of the linear portion into the x-axis gives the band gap of 3.20 eV [Figure 3(b)] which is consistent with the reported value in the literature.¹⁸

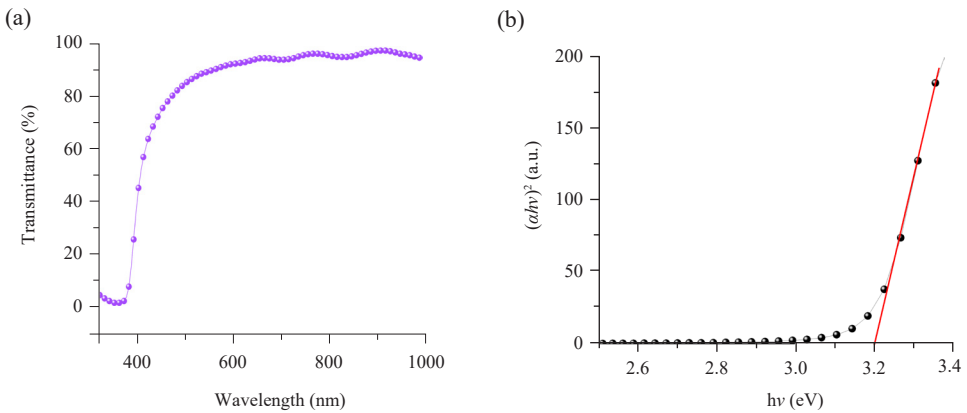


Figure 3: (a) UV-vis transmission spectrum and (b) band gap calculation of ZnO film.

3.3 Surface Morphology

The nature of the sensor surface is a vital factor in determining gas sensitivity towards various gases.^{5,19} Figure 4(a) shows the SEM micrograph of porous surface morphology of spin-coated ZnO film consisting of spherical grains. The compositional analysis of this film was performed using the energy dispersive x-ray (EDX) technique. Figure 4(b) reveals the atomic % of Zn and O content to be 52.33% and 47.67%, respectively.

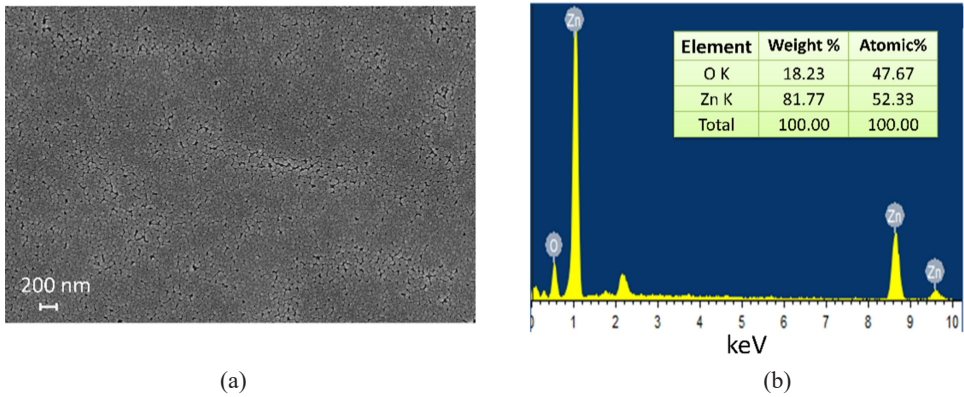


Figure 4: (a) SEM micrograph and (b) EDX spectrum with Zn and O content in ZnO film.

3.4 Sensor Performance

In the ambient atmosphere, the oxygen molecules are ionosorbed as O_2^- after extracting electrons from the conduction band of ZnO so that there is an increase in the width of the space charge (depletion) region and the height of the potential barrier on the grain boundaries of ZnO.²⁰ This growth of the depletion layer and barrier height is schematically shown in figure 5(a). The current measured at this state is termed as I_a which is measured by applying a fixed potential difference of 10 V across it. This voltage was kept affixed at 10 V as the baseline for the entire study. In the presence of reducing gas, such as ammonia (NH_3), electrons trapped by oxygen species return to the ZnO which causes the barrier potential height to decrease that concomitantly increasing the conductivity of ZnO. Figure 5(b) shows the liberation of electrons during the interaction of ammonia with O_2^- as $4NH_3 + 3O_{2(ads)}^- = 2N_2 + 6H_2O + 6e^-$ and decrease of the depletion layer.²¹ The current measured at this instance is denoted as I_g , current in gas. By evaluating the ratios of I_g/I_a , we can find out the sensing performance of ZnO-based gas sensors.¹²

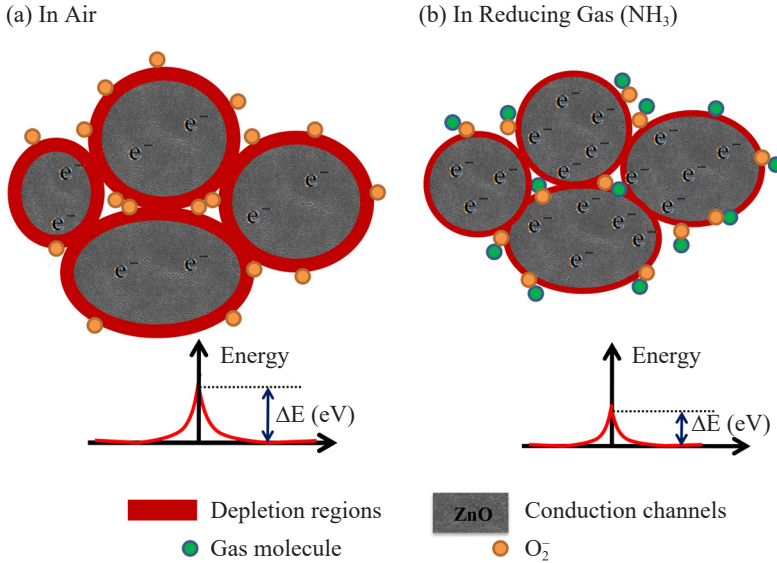


Figure 5: Illustration of the working mechanism of ZnO sensor (a) in the air (b) in reducing gas.

Figure 6(a) shows the response of the ZnO sensor ($I_g/I_a \sim 38.5$) towards 400 ppm of ammonia vapour for five cycles. Further, we investigated the sensing performance of the sensor towards different concentrations of ammonia vapour. Figure 6(b) shows the variation of gas response plotted against sensing time for various ammonia concentrations. We noticed the reduction in gas response efficacies with decreasing ammonia concentrations. The times needed to acquire 90% and 10% of maximum response after injection and ejection of the gas from the chamber are called response time and recovery times of the sensor, respectively. The response time always depends on the reaction rate of exposed gas with adsorbed oxygen species on sensing material, whereas, the recovery time depends on the rate of desorption of oxygen from the sensor surface after the vapour is ejected.²² Both response and recovery times may also depend on the sensor geometry. The inset of figure 6(b) shows the determination of response and recovery times of the ZnO sensor upon the exposure of ammonia vapour of 400 ppm. The response and recovery times are found to be 37 s and 90 s, respectively. To test the repeatability and stability of the sensing device, we repeated the same experiment with identical parameters for eight days and discovered the response to be constant at the value of ~ 38.5 , which showed the device to be highly consistent across each measurement [Figure 6(c)]. Figure 6(d) depicts the sensing response of the ZnO sensor towards various vapours including acetone, ethanol, isopropanol, methanol and ammonia. The

ZnO sensor shows prominent selectivity towards ammonia vapour in comparison to other vapours under study. This is attributed to the smaller kinetic diameter and low ionisation energy of ammonia. The ammonia vapour with a small kinetic diameter diffuses easily in the available pores of ZnO and leads to more adsorption sites which consequently increase the gas sensing response.^{23,24} For clarity, the molecular weight, kinetic diameter, and ionisation energy of various gas molecules are shown in Table 1.^{25,26} The results obtained in this work were compared with the reported sensitivities of ZnO based sensors prepared by different methods and presented in Table 2. The comparison shows that the sensitivity of spin-coated ZnO is better than reported values for similar systems prepared by other methods such as hydrothermal and spray pyrolysis at room temperature.

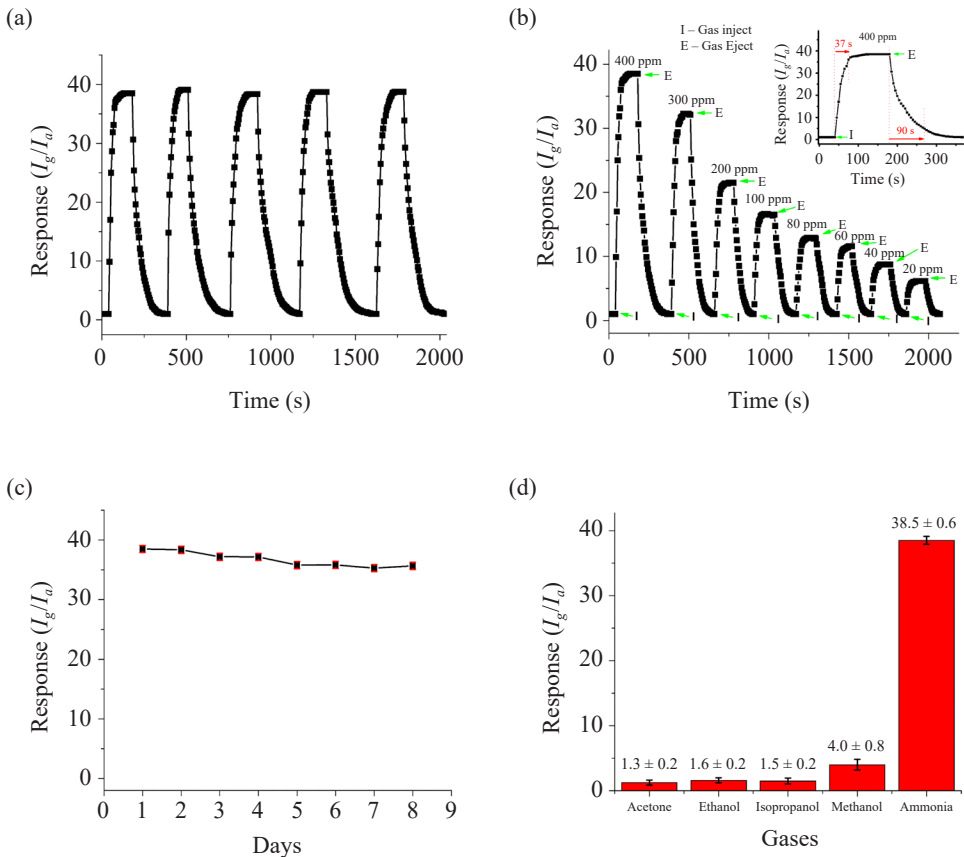


Figure 6: (a) Response curves with 400 ppm of NH_3 for five cycles, (b) response at different concentrations of ammonia (Inset: Calculation of response and recovery time with 400 ppm of NH_3), (c) repeatability, (d) selectivity measured at 400 ppm of various gases of ZnO sensor at room temperature.

Thus, we conclude that the results obtained herein using the spin coated ZnO film can be one of the best sensors for detecting low concentrations of ammonia vapour at room temperature.

Table 1. Kinetic diameter, molecular weight and ionisation energy of different molecules.

Vapour	Molecular weight	Kinetic diameter (nm)	Ionisation energy (eV)
Ammonia	17	0.26	10.18
Methanol	32	0.37	10.5
Ethanol	46	0.45	10.47
Acetone	58.05	0.46	9.69
Isopropanol	60.1	0.46	10.12

Table 2. Comparison of performance of ZnO based ammonia sensor of this work with reported works.

Materials	Method	Operating temperature (°C)	Ammonia (ppm)	Response (R_g/R_g or I_g/I_a) or sensitivity	Reference
ZnO Nanowire	Hydrothermal	350	200	4.2	[5]
			50	2.3	
			10	1.5	
In ₂ O ₃ -MgO with Pd- loaded TiO ₂ double layer	Thick film	530	300	25	[6]
SnO ₂	Spin coating	Room temperature	500	92.1%	[11]
Co-ZnO	Spray pyrolysis	Room temperature	100	3.48	[14]
Ni-ZnO	Spray pyrolysis	Room temperature	100	2.52	[15]
ZnO Nanorod	Hydrothermal	Room temperature	500	8%	[19]
ZnO Nanowire	SILAR	Room temperature	50	80.2	[24]
ZnO Grain	Spin coating	Room temperature	400	38.5 ± 0.86	This work
			20	6.1 ± 0.8	

4. CONCLUSION

To sum up, the structural characteristics showed the polycrystalline nature of ZnO with an average crystallite size of 27 nm. EDX results confirmed the highest purity of sensing material. SEM image showed porous morphology of ZnO film comprising of spherical grains. The optical band gap was found to be 3.2 eV which is consistent with the reported values. The gas sensing result showed the highest response towards ammonia among all tested gases. The

highest magnitude of the gas response towards 400 ppm of ammonia vapour was ~38.5. This result was compared to similar MOS for consistency and was found to be promising. The response and recovery times at 400 ppm of NH₃ were evaluated to be 37 s and 90 s, respectively. Interestingly, this work concludes that spin-coated ZnO films can be utilised for building a stable and low-cost gas sensor that can efficiently detect extremely low concentrations of ammonia vapour (as low as 20 ppm), which is reasonably below the OSHA recommended lower limit (35 ppm) of health hazard.

5. ACKNOWLEDGEMENTS

The authors would like to acknowledge International Science Program, Uppsala University, Sweden through the NEP-01 grant and University Grants Commission, Nepal for the support on instrumentation and consumables. We would also like to thank the Indian Institute of Technology (IIT), Roorkee, Uttarakhand, India which helped to obtain XRD, SEM and EDX spectra of ZnO thin films.

6. REFERENCES

1. Pearson, J. & Stewart, G. R. (1993). The deposition of atmospheric ammonia and its effects on plants. *New Phytol.*, 125, 283–305. <https://doi.org/10.1111/j.1469-8137.1993.tb03882.x>
2. Erisman, J. W. et al. (2008). How a century of ammonia synthesis changed the world. *Nat. Geosci.*, 1, 636–639. <https://www.nature.com/articles/ngeo325>
3. Timmer, B., Olthuis, W. & Berg, A. V. D. (2005). Ammonia sensors and their applications – a review. *Sens. Actuators B. Chem.*, 107(2), 666–677. <https://doi.org/10.1016/j.snb.2004.11.054>
4. Mani, G. K. & Rayappan, J. B. B. (2013). A highly selective room temperature ammonia sensor using spray deposited zinc oxide thin film. *Sens. Actuators B. Chem.*, 183, 459–466. <https://doi.org/10.1016/j.snb.2013.03.132>
5. Shao, F. et al. (2016). NH₃ sensing with self-assembled ZnO-nanowire μHP sensors in isothermal and temperature-pulsed mode. *Sens. Actuators B. Chem.*, 226, 110–117. <https://doi.org/10.1016/j.snb.2015.11.109>
6. Takao, Y. et al. (1994). High ammonia sensitive semi-conductor gas sensors with double-layer structure and interface electrodes. *J. Electrochem. Soc.*, 141, 1028–1034. <https://doi.org/10.1149/1.2054836>
7. Rambu, A. P., Nica, V. & Dobromir M. (2013). Influence of Fe-doping on the optical and electrical properties of ZnO films. *Superlattices Microstruct.*, 59, 87–96. <https://doi.org/10.1016/j.spmi.2013.03.023>
8. Hassan, M. M. et al. (2014). Fe dopants enhancing ethanol sensitivity of ZnO thin film deposited by RF magnetron sputtering. *J. Mater. Sci.*, 49, 6248–6256. <https://link.springer.com/article/10.1007/s10853-014-8349-2>

9. Srinivasulu, T., Saritha, K. & Reddy, K. T. R. (2017). Synthesis and characterization of Fe-doped ZnO thin films deposited by chemical spray pyrolysis. *Mod. Electron. Mater.*, 3(2), 75–85. <https://doi.org/10.1016/j.moem.2017.07.001>
10. Shrestha, S. P. et al. (2010). Properties of ZnO: Al films prepared by spin coating of aged precursor solution. *Bull. Korean Chem. Soc.*, 31, 112–115. <https://doi.org/10.5012/bkcs.2010.31.01.112>
11. Beniwal, A., Srivastava, V. & Sunny. (2019). Sol-gel assisted nano-structured SnO₂ sensor for low concentration ammonia detection at room temperature. *Mater. Res. Express*, 6(4), 046421. <https://iopscience.iop.org/article/10.1088/2053-1591/aafdd8/pdf>
12. Jha, R. K. et al. (2018). Enhanced gas sensing properties of liquid-processed semiconducting tungsten chalcogenide (WX_n, X = O and S) based hybrid nanomaterials. *IEEE Sens. J.*, 18(9), 20183494. <https://doi.org/10.1109/JSEN.2018.2810811>
13. Quan, S. Y., Tian, M. & Yang, L. M. (2009). Characterization of nanostructured ZnO thin films deposited by sol-gel spin coating. *Adv. Mater. Res.*, 79–82, 703–706. <https://doi.org/10.4028/www.scientific.net/AMR.79-82.703>
14. Mani, G. K. & Rayappan, J. B. B. (2015). A highly selective and wide range ammonia sensor-nanostructured ZnO: Co thin film. *Mater. Sci. Eng. B*, 191, 41–50. <https://doi.org/10.1016/j.mseb.2014.10.007>
15. Mani, G. K. & Rayappan, J. B. B. (2014). Selective detection of ammonia using spray pyrolysis deposited pure and nickel doped ZnO thin films. *Appl. Surf. Sci.*, 311, 405–412. <https://doi.org/10.1016/j.apsusc.2014.05.075>
16. Pramod, N. G. & Pandey, S. N. (2014). Influence of Sb doping the structural, optical, electrical and acetone sensing properties of In₂O₃ thin films. *Ceram. Int.*, 40(2), 3461–3468. <https://doi.org/10.1016/j.ceramint.2013.09.084>
17. Goh, E. G., Xu, X. & McCormick, P. G. (2014). Effect of particle size on the UV absorbance of zinc oxide nanoparticles. *Scripta Mater.*, 78–79, 49–52. <https://doi.org/10.1016/j.scriptamat.2014.01.033>
18. Nunes, P., Fortunato, E. & Martins, R. (2001). Influence of the post-treatment on the properties of ZnO thin films. *Thin Solid Film.*, 383(1–2), 277–280. [https://doi.org/10.1016/S0040-6090\(00\)01577-7](https://doi.org/10.1016/S0040-6090(00)01577-7)
19. Ang, W. et al. (2011). Room-temperature NH₃ gas sensor based on hydrothermally grown ZnO nanorods. *Chinese Phys. Lett.*, 28(8), 080702. <https://doi.org/10.1088/0256-307X/28/8/080702>
20. Yu, A. et al. (2011). Micro-lotus constructed by Fe-doped ZnO hierarchically porous nanosheets: preparation, characterization and gas sensing property. *Sens. Actuators B Chem.*, 158, 9–16. <https://doi.org/10.1016/j.snb.2011.03.052>
21. Dey, A. (2018). Semiconductor metal oxide gas sensors: A review. *Mater. Sci. Eng. B*, 229, 206–217. <https://doi.org/10.1016/j.mseb.2017.12.036>
22. Hongsith, N. et al. (2010). Sensor response formula for sensor based on ZnO nanostructures. *Sens. Actuators B Chem.*, 144, 67–72. <https://doi.org/10.1016/j.snb.2009.10.037>

23. Ozawa, K. et al. (2002). Adsorption state and molecular orientation of ammonia on ZnO (studied by photoelectron spectroscopy and near-edge X-ray absorption fine structure spectroscopy. *J. Phys. Chem. B*, 106(36), 9380–9386. <https://doi.org/10.1021/jp0205970>
24. Anasthasiya, A. N. A. et al. (2018). Adsorption property of volatile molecules on ZnO nanowires: computational and experimental approach. *Bull. Mater. Sci.*, 41(4), 1–7. <https://doi.org/10.1007/s12034-017-1538-2>
25. Zhu, G. et al. (2008). FAU-type zeolite membranes synthesized by microwave assisted in situ crystallization. *Mater. Lett.*, 62(28), 4357–4359. <https://doi.org/10.1016/j.matlet.2008.07.026>
26. Goel, S. et al. (2012). Synthesis and catalytic properties of metal clusters encapsulated within small-pore (SOD, GIS, ANA) zeolites. *J. Am. Chem. Soc.*, 134(42), 17688–17695. <https://doi.org/10.1021/ja307370z>